

Temperature Distribution of Particles in a Laser Beam

V. P. Lykhoshva¹, A. N. Tymoshenko¹, L. V. Mosentsova¹, V. V. Savin² and D. V. Schitz^{2*}

* dschitz@kantiana.ru

Received: September 2017 Accepted: January 2018

¹ Physics-Technological Institute of Metals and Alloys of the National Academy of Science of Ukraine, Ukraine.

² Immanuel Kant Baltic Federal University, Russia.

DOI: 10.22068/ijmse.15.1.1

Abstract: The particle temperature distribution depending on the laser radiation power and the particle's trajectory and velocity were studied. The uneven heating of particles moving in the laser radiation field was identified. The regimes of laser heating without melting, with partial melting, and with complete particle melting were considered.

Keywords: Metal Particles, Heating, Laser Beam, Modeling of Temperature Distribution.

1. INTRODUCTION

Using dispersion materials in deposition, sputtering, and similar procedures gained wide currency in science and technology [1, 2]. Different heating sources – laser, plasma, electron beams – are used in the process. In many cases, it is important to be aware of the changes in the particle temperature at different heating intensity depending on the particle trajectory, velocity, spin, and heating time. It is difficult to perform a direct measurement of a moving particle's temperature in a thermal field. This leads to a number of insurmountable obstacles. Therefore, researchers use various numerical methods to accurately calculate temperature distribution both on the surface and inside the particle. To simplify the calculation, it is assumed [3-5] that, due to rotation, the particle is heated evenly, whereas uneven heating resulting from the change of trajectory is not taken into account. However, a number of processes require a clear understanding of changes in the particle temperature at different thermal loads and heating times. This study aims to examine the temperature field of a particle moving in a laser irradiation zone at different velocities without rotation and with rotation acquired through a collision with nozzle walls.

In most cases the formation of a composite material require the introduction of particles either into the area of coating development

during melting and sputtering or into the melt through a tuyere or nozzle. Hence, there is a need to study the movement of particles in a tuyere in a laser flow.

2. EXPERIMENTAL PROCEDURE

In most cases the formation of a composite material require the introduction of particles either into the area of coating development during melting and sputtering or into the melt through a tuyere or nozzle. Hence, there is a need to study the movement of particles in a tuyere in a laser flow.

The most widespread tuyere (Fig. 1) was used for the formation of composite materials and their melting by laser irradiation. The tuyere structure includes a transportation channel 2 designed to introduce particles into a laser irradiation zone. The inclination angle of the transportation channel was chosen based on the geometrical possibility of a single collision with a nozzle diffuser wall for most particles. Moreover, in channel 1, through which a laser beam is directed, the pressure of inert gas equals that in the transportation channel.

A lens of a focal length $F=400$ mm and a focal spot diameter of 2 mm was used in the study. The focus of the laser radiation is moved to the tuyere neck area so that the particles are laser-treated in both focal and extra-focal areas.

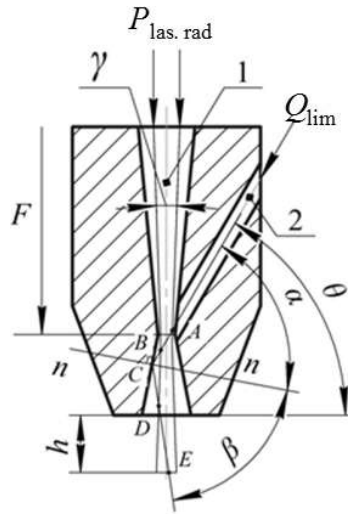


Fig.1. Laser tuyere for introducing and heating particles: 1 – gas laser channel, 2 – powder transportation channel (AB and DE are the particle trajectories in the laser radiation field before and after the collision with the nozzle wall, F - is focal length, α particle impact angle, β - particle rebound angle, γ - laser beam aperture angle, θ - inclination angle of the particle transportation channel, n - n - the line perpendicular to the tuyere diffuser passing through the point of particle collision with the tuyere wall, h - the distance between the tuyere and the target (melt surface), Q_{lim} – flow of particles, $P_{las. rad}$ – laser power)

The calculation assumes that spherical particles of a diameter of 500 μm placed in the tuyere move in the laser flow without colliding with each other collide only once with a tuyere wall.

The power of laser radiation was chosen so that, during the movement prior to the collision with the nozzle wall (segment AC in Fig. 1), the particle's temperature does not exceed that of melting, whereas further movement in the laser radiation field ensures particle heating to the melting and higher temperatures as a result of the time the particle spends in the laser radiation field.

At the first stage, the distance between the tuyere nozzle exit and the final point of movement is assumed to be 10 mm. The initial velocity of particle introduction into the tuyere is changed from 1 to 25 m/s. The particle material is low-carbon steel or carbonyl iron (carbon content $\leq 0.03\%$).

3. SIMULATION MODEL

The trajectory of movement and the time spent by the particle in the laser field was identified

using methods of numerical hydro- and gas dynamics and a two-phase ANSYS CFX mathematical model.

It is supposed that the particle travels along segments AB (Fig. 1) and DE with constant velocity V_1 and V_2 respectively. Within segment DE, it acquires a rotation ω after its collision with a nozzle diffuser wall. The time the particle spends in the laser radiation field is calculated as the ratio of distance to velocity.

The angular velocity of the particle is calculated using a system of Eq. (1):

$$\begin{cases} \frac{mV_1^2}{2} = \frac{mV_2^2}{2} + \frac{J\omega^2}{2}, \\ m\bar{V}_1 = m\bar{V}_2, \end{cases} \quad (1)$$

where V_1 is the initial velocity [m/s], V_2 - velocity after the collision with the nozzle diffuser wall [m/s], $J=2.5mR^2$ - the moment of inertia for the spherical particle [$\text{kg}\times\text{m}^2$], m - particle mass [kg], and ω - angular velocity of the particle [rad/s].

The system of equations given above makes it possible to establish a dependence of angular velocity ω on initial velocity V_1 , radius R , impact angle α , and rebound angle β :

$$\omega = \sqrt{\frac{5}{2} \frac{V_1}{R} \sqrt{1 - \left(\frac{tg\alpha}{tg\beta}\right)^2}} \quad (2)$$

The calculation of the particle's thermal field depending on the power of laser radiation and the particle's thermophysical parameters is conducted using the ANSYS Thermal software.

According to recommendations given in [6], the convective heat transfer is assumed at 200 W/s throughout the particle surface.

Instantaneous power density W_i is determined by the power of laser radiation P and instantaneous distance H_i from the focal place of laser radiation to the parallel plane of the particle's radial section according to:

$$\frac{\partial W_i(t)}{\partial t} = \frac{A \cdot P}{\pi \cdot t \cdot g^2 \frac{\gamma}{2}} \cdot \frac{\partial H_i(t)}{\partial t} \quad (3)$$

where: A is the particle's absorptivity and γ - the aperture angle of laser radiation (Fig. 1).

Power density throughout the exit area is assumed equal to the power density in the focal plane. The transfer of heat from the particle to the tuyere diffuser wall is not taken into account.

A continuous rotation of the particle is replaced with its impulsive turning motion. The

time of an impulse of turn τ is obtained using the formula:

$$\tau = \frac{\vartheta}{a_c n} = \frac{\omega R}{\omega^2 R} \cdot \frac{\alpha}{360^\circ} = \frac{\alpha}{360^\circ \omega} \quad (4)$$

where v is linear velocity [m/s], a_c - centrifugal acceleration [m/s²], n - the number of sectors ($n=360^\circ/\alpha$), ω - angular velocity of particle rotation [rad/s], and α - the turning angle [deg].

4. RESULTS AND DISCUSSION

Distribution of the particle's temperature fields within segment AB (Fig. 1) is modelled in view of the initial and boundary conditions. At the particle velocity of 1-25 m/s, particle heating can occur without surface melting (solid phase), with partial melting (liquid-solid phase), full melting (liquid phase), or partial vaporisation (liquid and gaseous phases) depending on the power of laser radiation.

The necessary values of the particle velocity and laser radiation power, at which the particle temperature does not reach the melting point within segment AB, are obtained. Fig. 2(a) shows that this condition is met at a velocity of 10-25 m/s and a power of 600-2200 W. At a

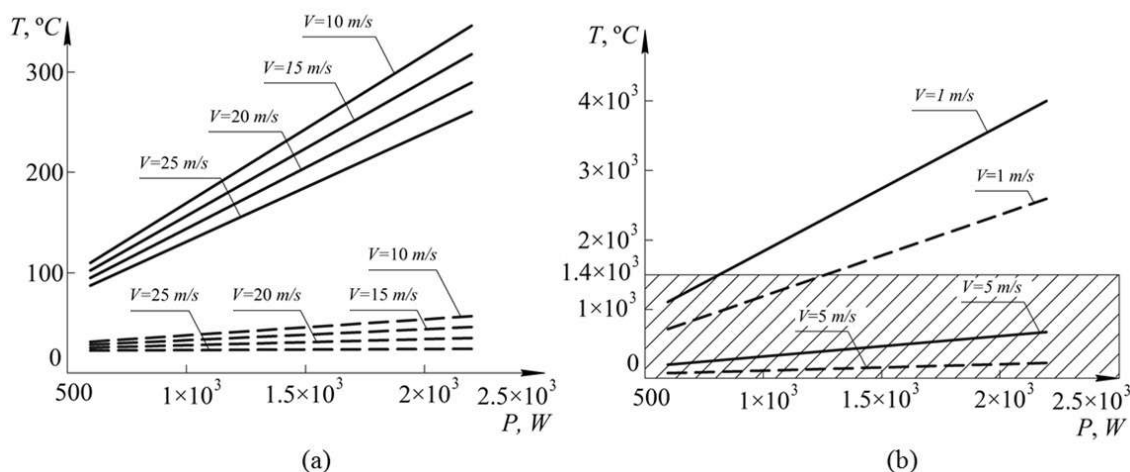


Fig. 2. Changes in the particle temperature depending on the laser radiation power and particle velocity: (a) - $V = 10-25$ m/s, (b) - $V = 1-10$ m/s. Solid lines - irradiated side of particle, dash lines - nonirradiated side of particle.

velocity of 1-10 m/s, the condition is met only within the hatched area (Fig. 2(b)). In particular, at a velocity of 1 m/s, this condition can be met only at a power of 600-800 W, at 2 m/s at a power of 600-1000 W, and at 3 m/s at 600-1500 W. At a velocity above 4 m/s, the condition is met at all the values considered. Above the hatched area, the particle temperature can reach the melting and even evaporation point.

The temperature difference $\Delta T = T_{\max} - T_{\min}$ between the most (T_{\max}) and the least (T_{\min}) heated particle area is taken as a parameter for estimating the non-uniformity of particle heating. In the case of a non-rotating particle (segment AC of the particle movement, Fig. 1), the most heated area is the one exposed to laser radiation, whereas the least heated area is that not exposed to radiation.

Let us consider changes in the particle temperature difference depending on its velocity within the range of 1-10 m/s at a fixed laser radiation power value (Fig. 3). As the velocity of the particle movement increases within this range at a laser radiation power of 2200 W, the temperature difference decreases from 1500 to 300 °C, whereas at the radiation power of 600 W, it reduces from 400 to 80 °C.

Therefore, within the velocity range of 1-10 m/s, the particle temperature difference is more sensitive to changes in the particle movement velocity in comparison to the impact of laser radiation power.

The same tests were conducted for the particle movement velocity range of 10-25 m/s. These parameters had the same effect on the temperature difference (Fig. 3), i.e. within this range of changes in the particle movement velocity, the temperature difference is more sensitive to changes in the laser radiation power in comparison with the particle movement velocity.

Within segments BC and CE (Fig. 1), the heating of the particle by laser radiation does not occur. The temperature field of the particle was calculated with regard to convective heat exchange with the environment. Within these segments, the particle collides with the nozzle diffuser wall and starts rotating; rotation changes the particle movement direction. Calculation of

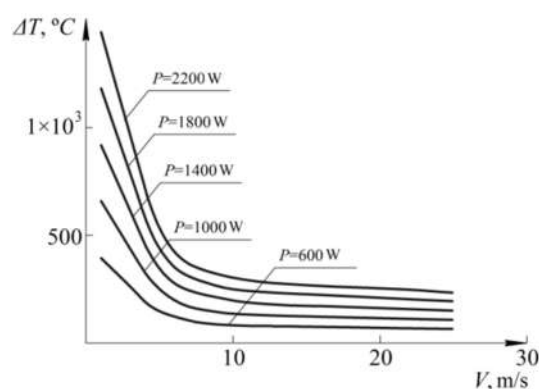


Fig. 3. Changes in the temperature difference of the particle heating depending on its velocity and the laser radiation power

the particle movement velocity and rotation is done according to Eq. (1) and (2).

As the particle collides with the diffuser prior to irradiation, it turns through a certain angle. The particle surface – which is later exposed to laser irradiation – is part of the irradiated area of segment AB and part of the non-irradiated area within segment CE. This serves as the initial data for further calculation of particle heating.

The particle trajectory suggests that its irradiation takes place until the final point specified by the parameter h is reached (Fig. 1). Within this segment, the particle makes $5/6$ of revolution at all velocities. One can also identify the area of the particle surface exposed to radiation throughout the segment. This – most heated – area accounts for $1/6$ of the particle surface.

Within segment DE, the particle surface temperature does not reach the melting point, i.e. it remains in the solid phase throughout the segment at a velocity of 3 m/s and a power of 600-1000 W, at a velocity of 5 m/s and a power of 600-1200 W (Fig. 4(a)), as well as within the velocity range of 10-25 m/s and a power of 600-2200 W (Fig. 4(b)). At a particle velocity of 1-5 m/s, heating without melting occurs in the diagonally hatched area (Fig. 4(a)).

In Fig. 4(a), full melting takes place in the vertically hatched area. In this area, the minimum particle temperature is above the liquidus point,

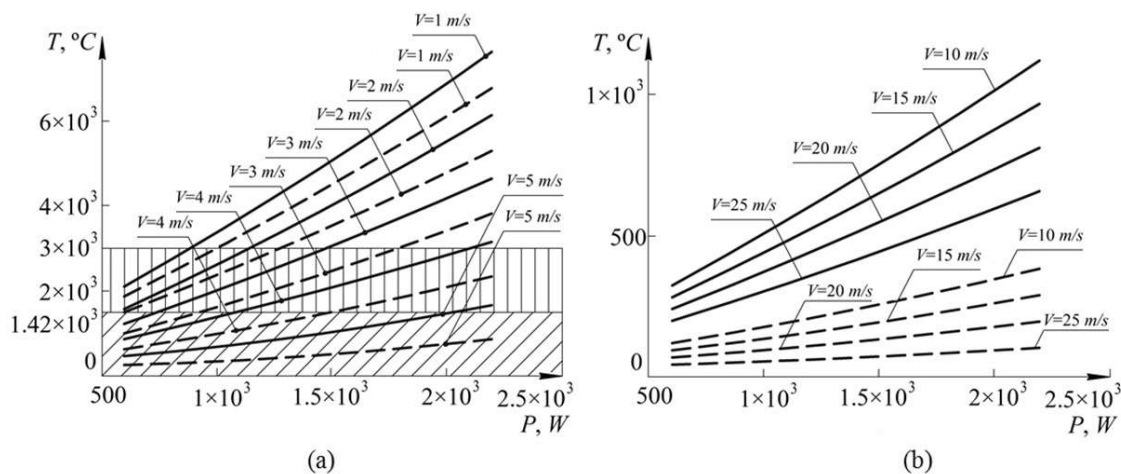


Fig. 4. Temperature changes depending on the laser radiation power and the particle velocity: (a) $V = 1-10$ m/s, (b) $V = 10-25$ m/s.

Solid lines - irradiated side of particle, dash lines - nonirradiated side of particle.

whereas the maximum temperature is below the evaporation point and the whole particle is in the liquid phase. Above this area, partial or complete evaporation takes place. This mode of laser irradiation is not acceptable in our case, since it results in the destruction of the particle.

A number of technologies using particle

heating require surface melting of the particle or its partial melting. Therefore, a condition of particular interest is the area at the interface of the liquid and solid phases, which corresponds to the power variation range of $700-850$ W at a particle velocity of 3 m/s, the power variation range of $1000-1500$ W at a velocity of 4 m/s, and

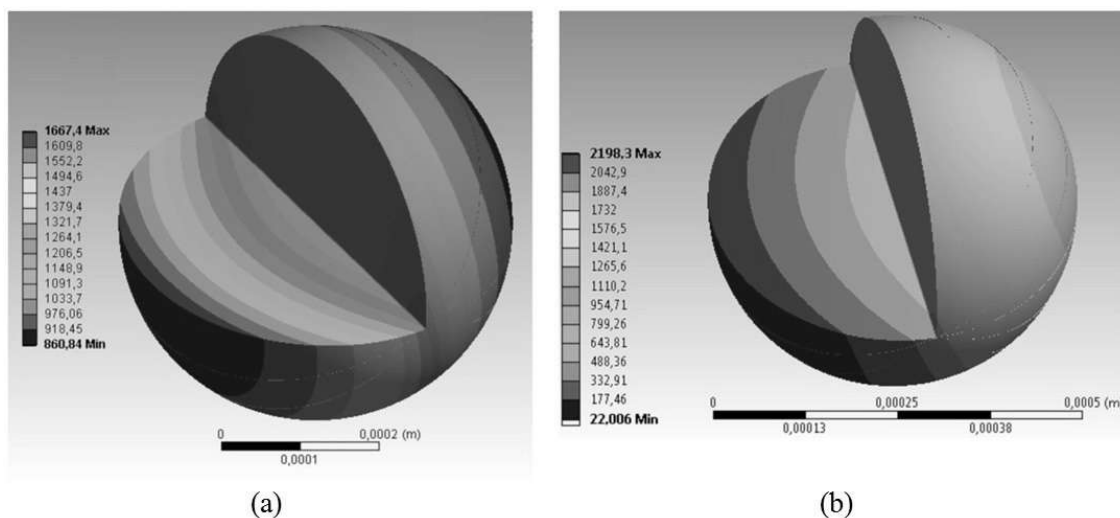


Fig. 5. Particle temperature distribution: (a) $V = 5$ m/s, $P = 2200$ W, (b) $V = 4$ m/s, $P = 1500$ W

the power variation range of 2100-2200 W at a velocity of 5 m/s (Fig. 4(a)).

The results of the mathematical modelling of particle melting for an initial velocity of 5 and 4 m/s and a laser radiation power of 2200 W are shown in Fig. 5. The area of particle melting accounts for approximately 30% of the surface in the first case (Fig. 5(a)) and for more than 90% in the second (Fig. 5(b)). Even when the particle rotation speed reaches 2500 and 3000 rev/min, the melt front remains almost flat, which does not make the uniform melting of the particle surface possible. However, the latter is not the case in a number of calculations [6], where, in the conditions of supposed particle rotation, laser irradiation heating is assumed as uniform with the surface melting and the core remaining solid.

A study of the uniformity of the rotating particle heating (Fig. 6) shows that changes in the temperature difference depending on the velocity can be approximated by a line, whose slope angle is determined by the function from laser radiation power.

It is established that as the velocity of the rotating particle increases from 1 to 25 m/s, for instance at a laser radiation power of 2200, the temperature difference changes from 960 to 550 °C and at 600 W from 235 to 160 °C (Fig. 6). Therefore, throughout the variation range of rotating particle velocity and radiation power, the power of laser radiation has a more pronounced effect on changes in the temperature difference.

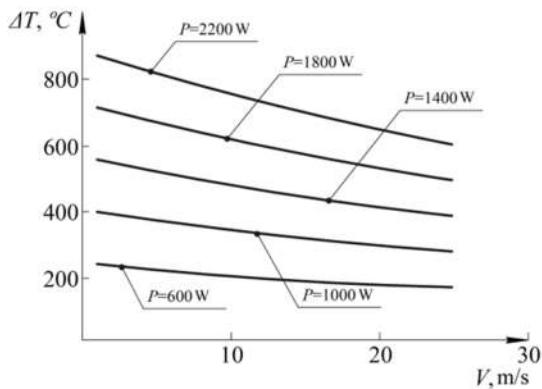


Fig. 6. Changes in the temperature difference of the rotating particle depending on the particle velocity and laser radiation power.

As the particle velocity and rotation speed increase, the temperature difference decreases. However, as it was mentioned above, the obtained rotation speed values are not sufficient for complete elimination of the temperature difference.

To assess the validity of the calculation results, a number of experiments were performed to obtain a composite material. Particles were introduced using the above-described tuyere and bronze melt. Particle heating was performed using a CO₂ laser with a wavelength of 10.6 μm. The rate of particle introduction was controlled by measuring gas exit velocity at the tuyere entrance. The particle material is low-carbon steel.

In the first experiment, particles are laser-treated in the area of heating without melting at 1000 W and V= 5 m/s. The sample study (Fig. 7(a)) shows that the particle-matrix interface consists of non-metallic inclusions remaining on the particle surface, which makes the interface rather broad and well-developed. Such parameters of particle heating can cause pores in the matrix material. The presence of non-metallic inclusions at the interface and pores is explained by the insufficient particle heating (without melting).

In the next experiment, particles are laser-treated in the area of partial melting at P= 2100 W and V= 5 m/s (Fig. 7(b)). In this case, the particle-matrix interface is broader; the unevenness of particle heating is visually manifested in the thickness of the interface. The particle form changes and becomes close to a sphere.

Within a higher temperature range of the particle heating (Fig. 7(c)), partial particle fragmentation is observed, which supposedly takes place in the most heated area of the particle. The particle-material interface becomes thinner.

If the particles are introduced into the melt in the liquid form, they are completely fragmented into smaller metal inclusions, which form finely divided composition (Fig. 7(d)).

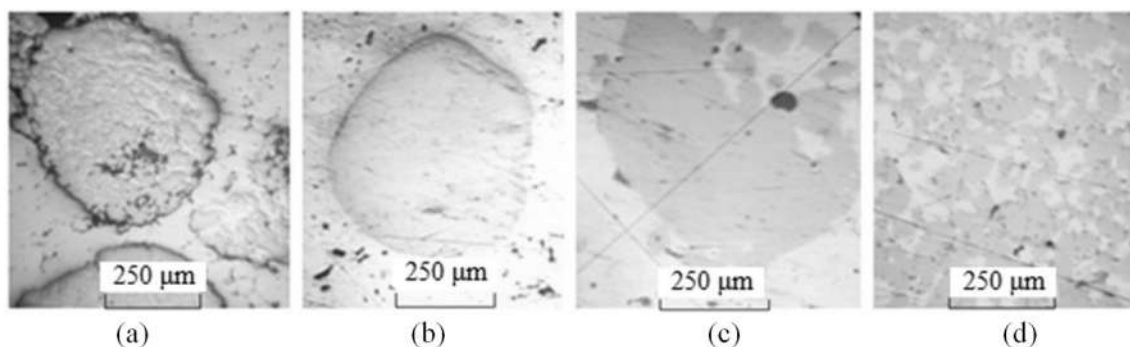


Fig. 7. The form and phase of particles in the metal matrix

5. CONCLUSIONS

It was established that a particle moving without rotation in a laser irradiation area with a non-uniform power density has a significant temperature difference reaching 1500 °C.

It was shown that a collision with the nozzle wall caused the rotation of the particle. However, the particle showed a full revolution only at a distance of at least 13 mm from the nozzle exit to the target (the melt surface). At a distance of 10 mm, as the experiment showed, the particle did not show a full revolution, resulted a temperature difference, whose maximum value was reduced to 960 °C as compared to a rotating particle.

Calculations and tests on the obtained composite material showed that despite a high velocity of particle rotation, the melt front remained almost flat and surface melting did not take place.

To obtain a reliable connection between a metal particle and a material matrix, the particle temperature should not exceed the melting point.

Variation ranges of the particle velocity and laser radiation power with partial surface melting are optimal modes for the formation of suspension melt and obtaining a reliable connection between the particle and the base material. This range also makes partial fragmentation possible, which is accompanied by the formation of smaller metal inclusions.

Provided liquid particles are introduction into the melt, emulsion areas may form.

ACKNOWLEDGMENTS

The study was supported by the Federal program and the Ministry of education and science of the Russian Federation (projects: No.14. 578.21.0252; No.3.5033.2017 and No.16 .4119.2017/PCh).

REFERENCES

1. Kruth, J. P., Levy, G., Flocke, F. and Childs, T. H. C., "Consolidation Phenomena in Laser and Powder-Bed Based Layered Manufacturing". *CIRP Annals - Manufacturing Tech.* 2007, 56(2), 730-759.
2. Gu, D. D., Meiners, W., Wissenbach, K. and Poprawe, R., "Laser additive manufacturing of metallic components: materials, processes and mechanisms". *Int. Materials Reviews.* 2012, 57(3), 133-164.
3. Borisov, Yu., Bushma, A. and Krivtsov, I., "Modeling of motion and heating of powder particles in laser, plasma, and hybrid spraying". *J. of Thermal Spray Technology.* 2006, 15(4), 553-558.
4. B. Mirzakhani, H. Arabi, S. H. Seyedein, M. R. Aboutalebi, M. T. Saleh and Sh. Khoddam, "Computer aided optimization of specimen geometry of hot torsion test to minimize microstructure nonhomogeneity and temperature gradient before deformation." *Iranian Journal of Materials Science and Engineering.* 2009, 6(3), 35-43.

5. Pustovalov, V. K., "Theoretical study of heating of spherical nanoparticle in media by short laser pulses". *Chem. Phys.* 2005, 308, 103-108.
6. Byshma, A. I. and Krivtsun, I. V., "Modelling of laser heating of the fine ceramic particles" *Proceedings of the IV Europ.Conf. on Laser Treatment of Materials (ECALT'92)*, Germany, Göttingen, 1992, 719-723.